PALEOCEANOGRAPHY, VOL. 23, PA4205, doi:10.1029/2008PA001593, 2008

Northern timing of deglaciation in the eastern equatorial Pacific from alkenone paleothermometry

Athanasios Koutavas[1,2] and Julian P. Sachs[3]

Received 14 January 2008; revised 7 July 2008; accepted 12 August 2008; published 22 October 2008.

[1] The equatorial cold tongue (ECT) of the eastern Pacific is the most dynamic ocean region in the world's tropics and sets the tempo for global climate anomalies arising from El Niño–Southern Oscillation (ENSO) events. This region's deglaciation history and relationship with north and south polar climates remains poorly understood, impeding integration of tropical Pacific ocean-atmosphere dynamics and ENSO variability in our understanding of glacial cycles. Here we present alkenone reconstructions of sea surface temperature (SST) across the last glacial termination from five ECT cores east of the Galapagos Islands. A composite index of SST based on these demonstrates strong temporal affinity with the two-step deglaciation of the Northern Hemisphere, composed of two distinct warming steps at the beginning of the Bölling and the end of the Younger Dryas intervals. Within dating uncertainty, warming in the ECT began in phase with the Bölling excursion, was followed by a 2–3 ka plateau, and resumed with a second pulse at the end of the Younger Dryas. On the basis of our reconstructions, about two thirds of the warming materialized at or after the end of the Younger Dryas, implying a marked delay in the region's response to deglaciation. The results challenge the prevailing paradigm that ECT deglacial history conforms to an Antarctic timing, commonly attributed to advection from the Southern Ocean through an interior oceanic link, or to synchronous response of both regions to CO_2 forcing. Our results emphasize instead the role of dynamical adjustments linked to Northern Hemisphere processes, most likely transmitted through the atmosphere.

Citation: Koutavas, A., and J. P. Sachs (2008), Northern timing of deglaciation in the eastern equatorial Pacific from alkenone paleothermometry, *Paleoceanography*, *23*, PA4205, doi:10.1029/2008PA001593.

1. Introduction

[2] The eastern tropical Pacific is unique within the tropical oceans for its ability to undergo fast dynamic adjustments and remarkably large sea surface temperature (SST) changes with a total amplitude of 10°C or higher. This variability arises from strong coupling between the atmosphere and surface ocean in the presence of a shallow and steep thermocline [*Mitchell and Wallace*, 1992]. Poleward Ekman transports on either side of the equator are balanced by equatorial upwelling bringing cool, nutrient-rich waters to the surface. SST in this region is closely monitored today and used to describe the state of the El Niño–Southern Oscillation (ENSO), the largest source of interannual climate variability on the planet. Paleoceanographic records of SST from this region are valuable for understanding its role in glacial-interglacial cycles and in the abrupt millennial-scale Dansgaard-Oeschger (D-O) oscillations that punctuated the last glacial period [*Dansgaard et al.*, 1993]. The tropical Pacific is considered a potential climatic "globalizer" that may accomplish the rapid, widespread propagation of abrupt climate changes observed in the northern hemisphere [*Cane*, 1998; *Clement and Cane*, 1999] but compelling evidence for this idea has yet to emerge [*Broecker*, 2003].

[3] The timing of deglacial temperature change in this region and its relation to northern or southern polar deglaciation can provide important constraints on the mechanisms linking the tropical Pacific with high-latitude and global climate changes. On the basis of evidence from Mg/Ca thermometry in planktonic foraminifera, it has been argued that tropical Pacific SSTs have covaried with Antarctic and Southern Ocean temperatures, implying a fundamental climate connection between these two regions [*Lea*, 2004; *Lea et al.*, 2006; *Pena et al.*, 2008]. This connection is envisioned to operate via a direct ocean link (often termed the "oceanic tunnel") involving subduction of intermediate and mode waters in the subantarctic region and resurfacing in the equatorial Pacific after transit along the Equatorial Undercurrent (EUC). Transmission of extratropical climate signals to the tropical Pacific via this mechanism has been studied in models [*Liu and Yang*, 2003] and is considered an important pathway linking the tropics with southern high latitudes during glacial-interglacial cycles [e.g., *Spero and Lea*, 2002]. Alternatively, synchronization of tropical Pacific and Antarctic climate records may result from direct response of each region to greenhouse forcing (primarily CO_2) a mechanism independent of the oceanic connection, but possibly operating in

[1]Department of Engineering Science and Physics, College of Staten Island, City University of New York, New York, USA.
[2]Lamont-Doherty Earth Observatory, Earth Institute at Columbia University, Palisades, New York, New York, USA.
[3]School of Oceanography, University of Washington, Seattle, Washington, USA.

0883-8305/08/2008PA001593$12.00

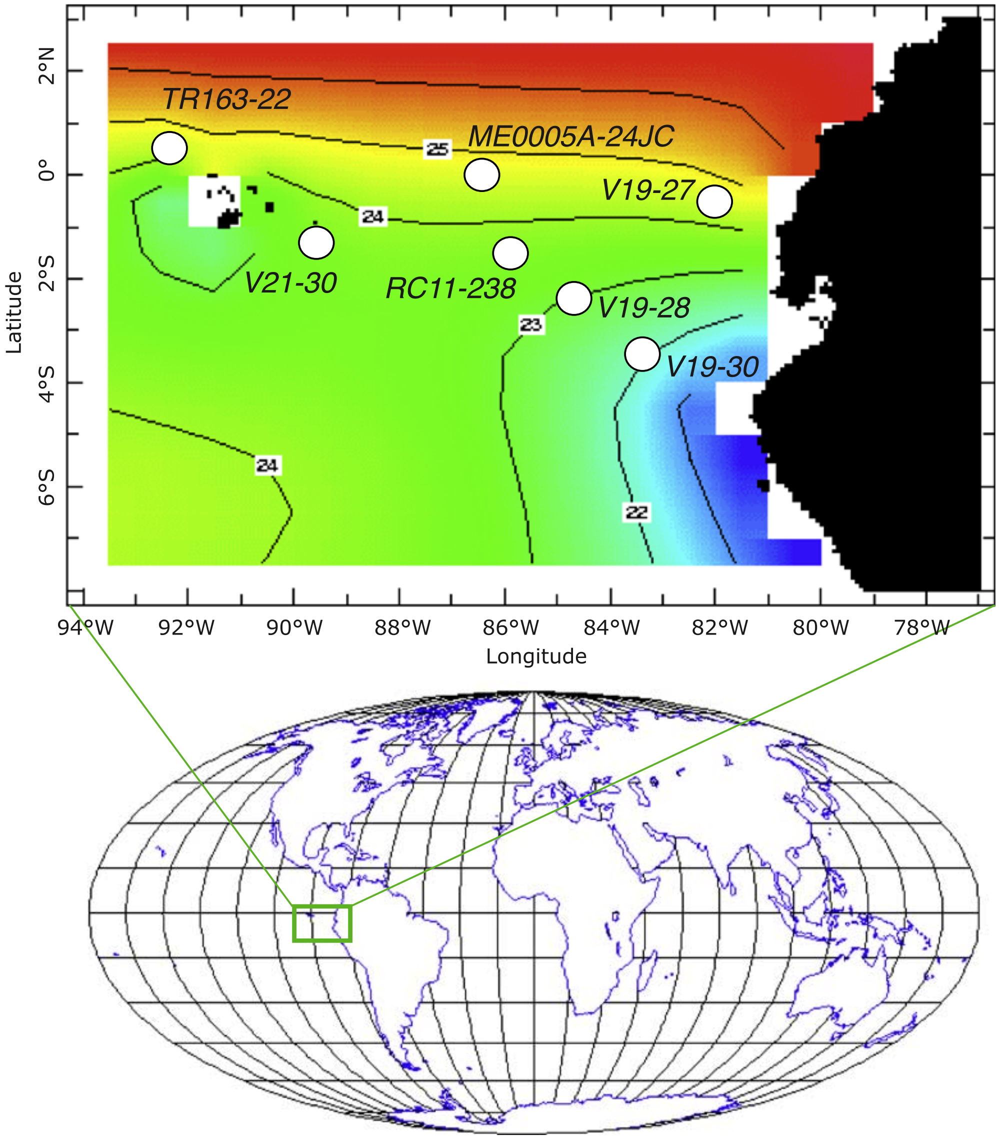

Figure 1. Locations of the studied sites in the eastern Pacific equatorial cold tongue. Site coordinates are given in Table 1. The background SST distribution corresponds to annual mean conditions from *Locarnini et al.*'s [2006] data.

tandem. The strength and overall significance of these processes (the oceanic tunnel and the radiative response) in shaping eastern Pacific SST variability must be weighed against the region's remarkable potential for dynamic adjustments due to coupled ocean-atmosphere interactions affecting the depth of the thermocline, the strength of wind-driven upwelling, and ENSO variability [*Wang and Fiedler*, 2006]. Such adjustments could overwhelm slowly varying climate signals transmitted via ocean advection or due to radiative effects, and could feed back on global climate in similar manner to modern-day interannual ENSO events.

[4] Evidence for abrupt hydrologic changes during the last glacial period has emerged recently in well-resolved records from the northeastern tropical Pacific offshore Central America [*Benway et al.*, 2006; *Leduc et al.*, 2007], a region dominated by warm SSTs and seasonally high precipitation under the Intertropical Convergence Zone (ITCZ). These hydrologic variations mimic the millennial-scale D-O oscillations that dominate northern hemisphere climate variability, and demonstrate that a northern climate signal extended into the northeast tropical Pacific affecting surface ocean hydrology. Closer to the equator, evidence from alkenone thermometry has revealed deglacial SST changes correlative with Heinrich Event 1, and the Younger Dryas cooling in the North Atlantic [*Kienast et al.*, 2006; *Pahnke et al.*, 2007]. Because of the complex oceanographic structure of the eastern equatorial Pacific, the presence of a sharp equatorial front (Figure 1), and the distinct set of dynamics that distinguish the equatorial cold tongue (ECT) south of the equator from the broader region, it remains unclear whether the northern style signal extended south of the equator, or whether by virtue of its strong link with the

Table 1. Coordinates of the Eastern Pacific Cores Discussed in This Study[a]

Core	Latitude	Longitude	Depth (m)	Annual Mean SST (°C)	Maximum SST (°C)	Minimum SST (°C)	Core Top $U_{37}^{K'}$ SST (°C)
V19–27	0°28′S	82°4′W	1373	24.40	25.39	23.55	26.54
V19–28	2°22′S	84°39′W	2720	22.88	25.68	20.90	24.04
V19-30	3°23′S	83°31′W	3091	22.10	25.21	19.79	22.73
V21-30	1°13′S	89°41′W	617	23.50	26.65	21.35	24.76
RC11-238	1°31′S	85°49′W	2573	23.57	25.99	21.92	24.43
ME0005A-24JC	0°1.3′N	86°27.8′W	2941	25.04	26.51	24.08	24.91
TR163-22	0°30.9′N	92°23.9′W	2830	24.40	26.84	22.52	-

[a]Also given are the annual mean, maximum, and minimum SST from *Locarnini et al.*'s [2006] data, as well as the core top $U_{37}^{K'}$ reconstructed temperature for each site. SST, sea surface temperature.

Southern Ocean the ECT responded instead on an Antarctic timing.

[5] Evaluation of the relative role of these processes requires well-dated high-resolution SST records in key regions within the tropical Pacific, foremost among them the ECT. Moreover, the oceanographic complexity of the region places increasing demands for replication and convergence of results from multiple sites to bolster confidence in reconstructed climate patterns.

2. Material and Methods

[6] Our study is based on alkenone unsaturation thermometry ($U_{37}^{K'}$) in five cores (RC11–238, V19–27, V19–28, V19–30, and V21–30) from the easternmost, coldest and highly dynamic part of the eastern Pacific ECT (Figure 1 and Table 1). The sites are strategically located to detect dynamic effects due to wind-forced divergent upwelling. Moreover, because of the local upwelling of deep EUC layers originating in the subantarctic region, they are equally well positioned to evaluate the importance of the oceanic tunnel as a conduit of climate signals from the Southern Ocean.

[7] Alkenone analysis followed laboratory protocols previously published by *Sachs and Lehman* [1999] and summarized as follows: approximately 1–3 g of sediment was gently crushed and mixed with an equal amount of sodium sulfate (a dispersing and drying agent). Following addition of a recovery standard (2 μg of Ethyl triacontanoate in 20% acetone in hexane), samples were packed in steel cells and extracted with dichloromethane at 150°C and 1500 psi using a DIONEX ASE 200 accelerated solvent extractor. Total lipid extracts were dried under a stream of N_2 gas, transferred to 2-mL autosampler vials and redissolved in 400 μL toluene containing 2 μg of *n*-hexatriacontane (*n*-C_{36}, a quantitation standard). Samples were derivatized with bis(trimethylsilyl)trifluoroacetamide for 1 hour at 60°C and alkenones (C_{37} methyl ketones) were quantified by capillary gas chromatography on an Agilent 6890N with a Chrompack CP-Sil-5 column (60 m by 0.32 mm inner diameter, 0.25 μm film thickness), a programmable temperature vaporization inlet in solvent-vent mode, and flame ionization detector. The oven was programmed from 110°C to 270°C at 40°C/min followed by a temperature increase of 2°C/min to 320°C, and an 18 min isothermal period. Temperature estimation is based on the calibration equation of *Prahl et al.* [1988]. Analytical precision based on repeat analyses of a Bermuda Rise sediment standard is ±0.25°C (1 standard deviation).

[8] Age control on RC11–238, V19–27, V19–28 and V21–30 is based on ^{14}C ages listed in the paper by *Koutavas and Lynch-Stieglitz* [2003]. The age model of V19–30 is based on the paper by *Shackleton* [2000].

3. Results

3.1. Alkenone SSTs

[9] The alkenone SST reconstructions from our five sites are shown in Figure 2 alongside benthic δ^{18}O stratigraphies from each core, and are plotted versus age in Figure 4a. With one exception, the method yields late Holocene SST estimates within 0.7–1.3°C of the modern annual mean SST from *Locarnini et al.*'s [2006] data (Figure 1 and Table 1). This is within the ±1.5°C standard error of the global core top calibration of the $U_{37}^{K'}$ paleothermometer [*Müller et al.*, 1998] indicating that the results are consistent with the core top database. The one exception is core V19–27, which gives late Holocene SST values 1.5–2.0°C higher than the modern mean, although average Holocene SSTs are ~1°C higher. As a whole the data suggest that the alkenone method somewhat overestimates annual mean temperature in this region, possibly indicating a modest warm season bias in the production and sedimentary flux of the alkenones. The primary alkenone producer in the open ocean is the coccolithophorid *Emiliania huxleyi*, which is known to produce midlatitude blooms under conditions of stratified, low-salinity, silicate-depleted waters, often following relaxation of upwelling events [*Tyrrell and Taylor*, 1996; *Tyrrell and Merico*, 2004]. Although the specific ecologic niche of *E. huxleyi* in the cold tongue province is not known, such conditions would locally correspond with the warm season of December–April, and might explain the warm bias in the alkenones. Our results are consistent with a recent comparison of $U_{37}^{K'}$ values between core top sediments and overlying surface waters which found a systematic positive bias in the former [*Conte et al.*, 2006]. This bias is smallest (0–2°C) in the 22–26°C temperature range corresponding with our site locations, suggesting that whatever its origin, its influence on reconstructed $U_{37}^{K'}$ temperature is relatively small.

[10] Downcore data variations among the five sites show strong similarities and also some notable differences (Figure 4a). The profiles from V21–30 and V19–27 are very similar and display the smallest glacial-interglacial (G-I) amplitudes of 1.5° ± 0.5°C. The two deepest and more southerly neighboring cores, V19–28 and V19–30, have

somewhat higher G-I amplitudes of 2–2.5°C and show consistent variations back to 15 ka but diverge earlier. Given the proximity of these two sites (Figure 1) and the low signal-to-noise ratio in V19–28 below ~15 ka, we suggest V19–30 is the more reliable reconstruction. Finally, RC11–238 records a larger deglacial SST amplitude of 2.8°C, however the late Holocene section of this core was not recovered. These amplitudes are comparable to alkenone results obtained from nearby lower-resolution records [*Liu and Herbert*, 2004; *Horikawa et al.*, 2006], and more recently from higher-resolution sites [*Kienast et al.*, 2006; *Pahnke et al.*, 2007].

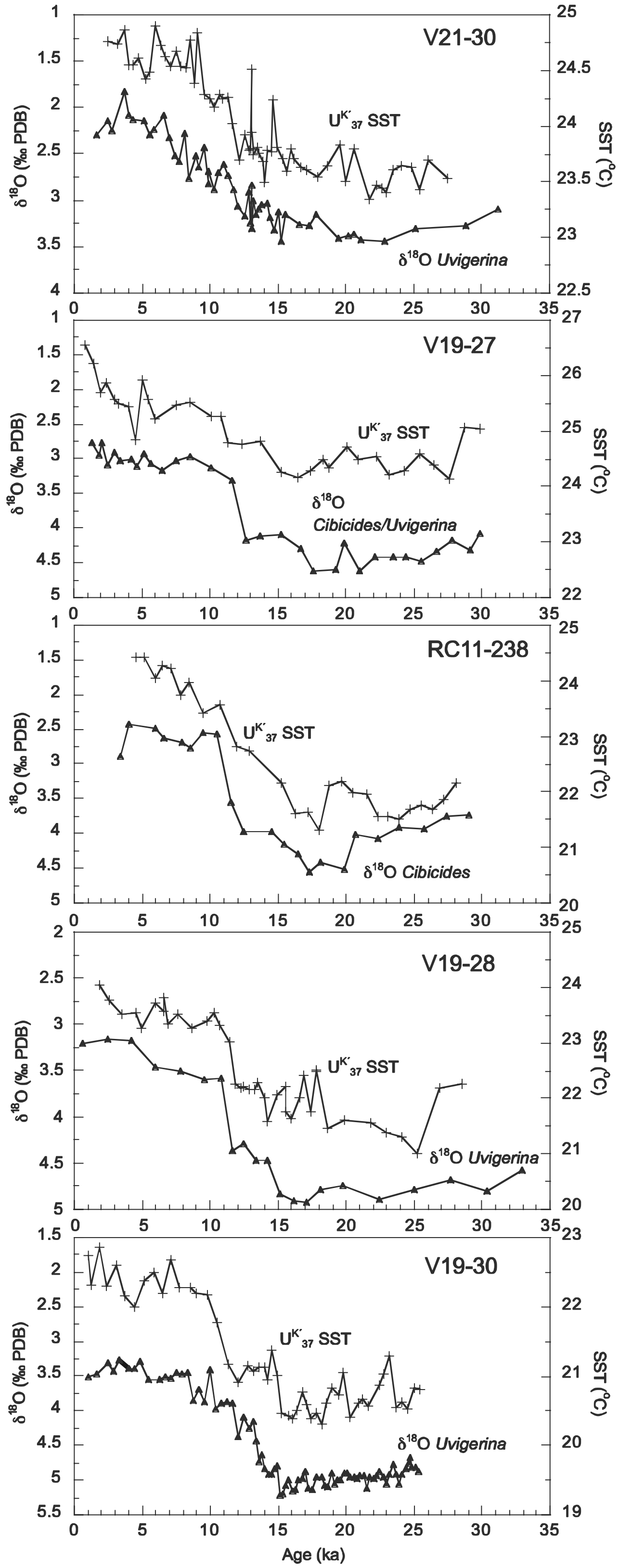

[11] Are the differences in amplitude among our five sites real and therefore indicative of changes in the regional oceanographic structure through time? Or are they the product of postdepositional alteration? In general the differences among the sites do not appear to be systematically related to their position across the SST gradient, proximity to the coastal region, latitude, or distance from the equator that might suggest a connection to a physical oceanographic process. We therefore lean toward the view that these differences are indicative of postdepositional artifacts at the local scale. This in turn raises the issue of reproducibility and reliability of the alkenone method. Alkenones reside in the fine sediment fraction and can be susceptible to postdepositional mobilization, horizontal advection, and redeposition by deep flows. This is chiefly a problem in sediment drifts, which is not the case in these sites. Therefore we anticipate sediment reworking to be of minor concern in our data although it cannot be entirely ruled out. We note that these five sites represent different depositional environments, with water depths ranging from 617 m to 3091 m and accumulation rates varying by a factor of three (4–13 cm/ka). Alkenone concentrations (Figure 3) also differ greatly among the sites especially during the late Holocene (range of 200–5000 ng/g). We surmise that the differences in recorded SST amplitude arise from combinations of factors related to different productivity regimes, accumulation rates, bioturbation, and perhaps minor lateral transport effects. Although these differences can confound the interpretation of the $U^{K'}_{37}$ results, they also offer one important advantage: sampling diverse depositional environments ensures that no single source of artifact dominates the entire data set, and in this sense we suggest that any nonclimatic effects in the records are likely random and would tend to cancel out when averaged.

3.2. Derivation of a Composite Standardized Alkenone SST Index

[12] With this rationale we focus attention on the overall pattern and timing of the deglaciation, which reveals evidence of overall consistency among the examined cores. One distinct example of this is the strong warming present in all records at ~11.5 ka (Figure 4a). Although resolution varies among sites, in each core this event marks the highest rate of warming in the last 30 ka, and amounts to a

Figure 2. Benthic $\delta^{18}O$ stratigraphies and alkenone temperature reconstructions for the five sites presented in this study. Benthic $\delta^{18}O$ data are from the following sources: V21–30 from *Koutavas* [2003], V19–27 from *Mix et al.* [1991], RC11–238 from *Faul et al.* [2000] and *Koutavas* [2003], V19–28 from *Ninkovich and Shackleton* [1975], and V19–30 from *Shackleton* [2000].

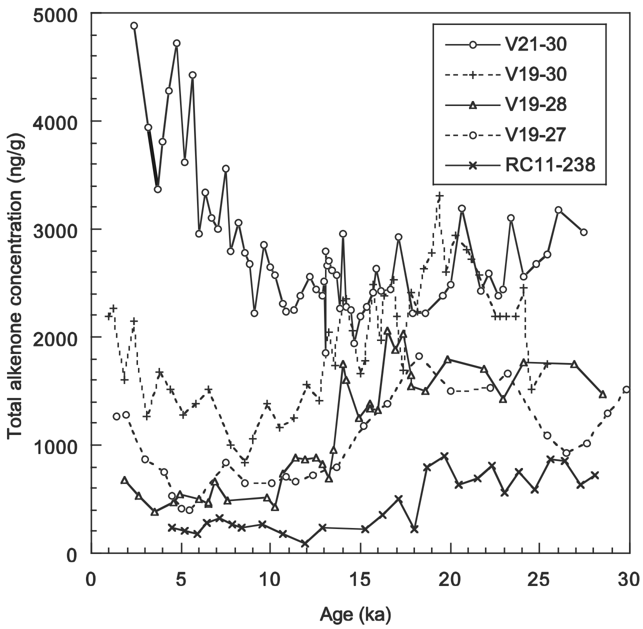

Figure 3. Total alkenone concentrations (ng/g) versus age for the five cores presented in this study.

significant fraction of the total G-I signal. To highlight the temporal coherency among the five $U^{K'}_{37}$ SST series we standardized the records to reflect departures from the mean rather than absolute values. The standardized series are shown in Figure 4b in the form of z-scores, calculated by subtracting the 0–30 ka mean and dividing by the standard deviation of each data series. Each standardized series thus has a mean of zero and unit standard deviation. This approach is similar to standardization of tree ring data, where a common climate signal is sought among multiple recording systems (e.g., individual trees or sites) each of which is often dominated by variable signals of nonclimatic origin [*Fritts*, 1976]. As with tree ring data, standardization and averaging of multiple series helps dampen random artifacts while amplifying the common climate signal.

[13] The standardized SST series in Figure 4b highlight those aspects of the deglaciation structure that are common to all sites. The main pattern consists of an essentially trendless glacial interval prior to ~15 ka with considerable fluctuations which do not appear systematic, a short, weak warming step at ~15 ka, a pause or plateau between 12–14 ka, and accelerated resumption of warming between 11 and 12 ka leading into the Holocene. The Holocene period itself is characterized by positive temperature trends in all of the cores in agreement with other alkenone records from the region [*Kienast et al.*, 2006; *Pahnke et al.*, 2007]. Mismatches in the standardized series (Figure 4b), for example over the interval of strong warming between 12 and 11 ka, likely reflect imperfect synchronization of the records due to age uncertainties. The two best ^{14}C dated sites (V21–30 and V19–28) are in near perfect alignment in this interval, followed closely by RC11–238, while the other two sites (V19–27 and V19–30) are offset by ~500 years. If the temporal mismatches in the 12–11 ka interval are indicative of the relative synchronization error among the records over their full length, we would estimate this error to be approximately ±500 years. On this ground, we derived a composite SST index series based on simple averaging of

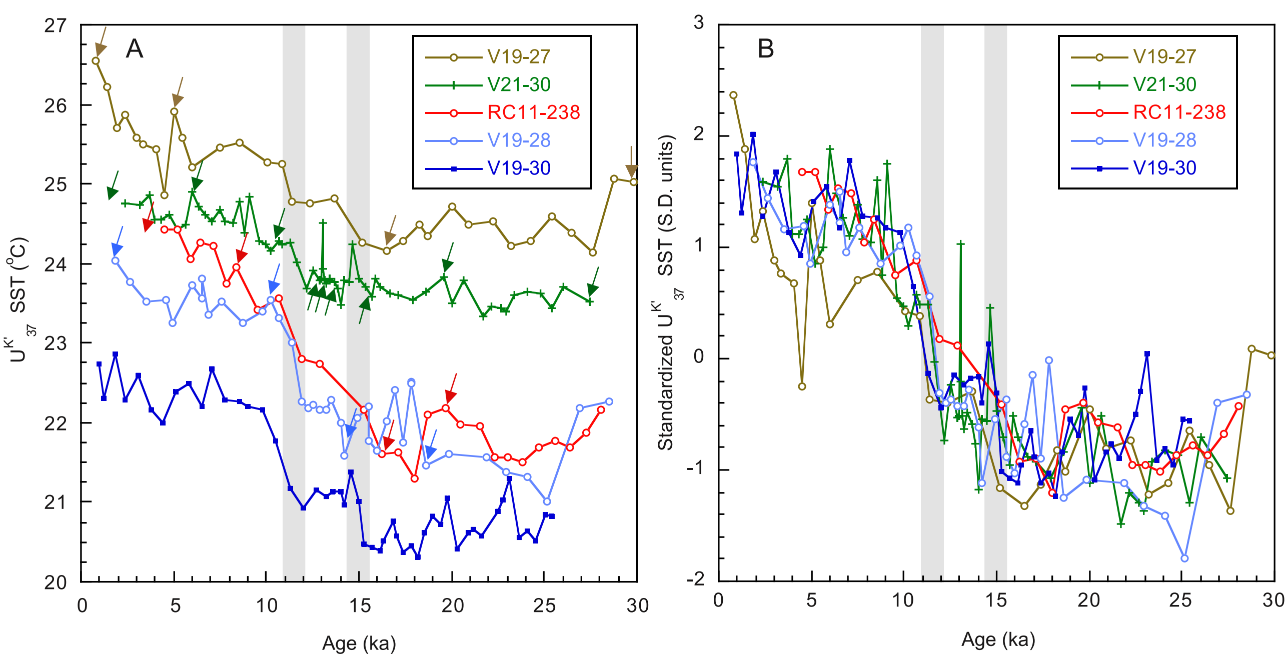

Figure 4. (a) Reconstructed alkenone SST histories for our five ECT cores plotted versus age. Arrows indicate ^{14}C ages used for age control. (b) Standardized dimensionless indices (standard deviation units) of the same alkenone time series. The gray bars in Figures 4a and 4b indicate our suggested timing of a first weak deglacial warming step at ~15 ka and a second stronger step at ~11.5 ka.

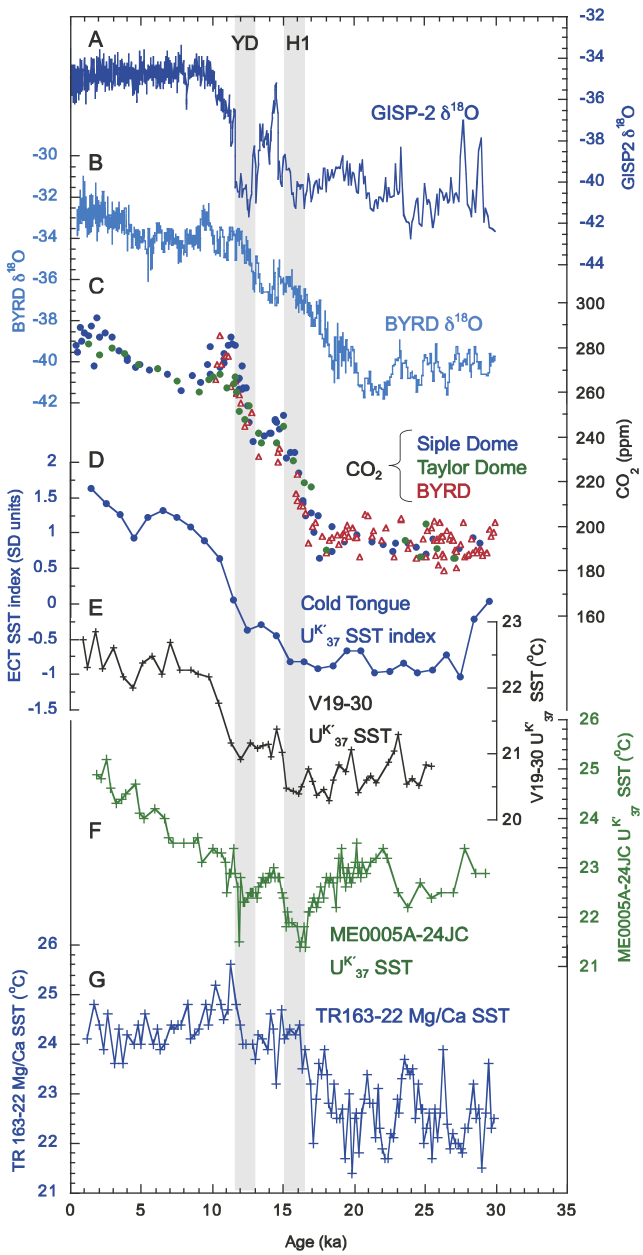

Figure 5. Comparison of alkenone and Mg/Ca-derived SST reconstructions from the equatorial cold tongue with polar ice core temperature records and atmospheric CO_2 over the last deglaciation. (a) Greenland Ice Sheet Project 2, Greenland, ice $\delta^{18}O$ [*Grootes and Stuiver*, 1997]; (b) BYRD, Antarctica, ice $\delta^{18}O$ [*Blunier and Brook*, 2001]; (c) Antarctic ice core CO_2 from Siple Dome [*Ahn et al.*, 2004], Taylor Dome [*Smith et al.*, 1999], and BYRD [*Blunier and Brook*, 2001]; (d) composite alkenone SST index (standard deviation units) based on the five records shown in Figure 4; (e) alkenone SST from site V19–30; (f) alkenone SST from site ME0005A-24JC [*Kienast et al.*, 2006]; and (g) *G. ruber* Mg/Ca SST from site TR163–22 [*Lea et al.*, 2006].

the standardized data of Figure 2 in 1000-year nonoverlapping windows, for comparison with climate records from the polar regions. The resulting dimensionless SST index is shown in Figure 5d, and represents a low-resolution best estimate of the deglacial SST progression in the broader ECT area east of the Galapagos. Because of the 1000-year averaging involved, age errors up to several centuries in individual cores would have little or no effect on the overall structure of the composite index.

3.3. Comparison With Polar Temperatures and CO_2

[14] In Figure 5 we compare the ECT SST index to polar deglaciation records from the Greenland Ice Sheet Project 2 (GISP-2) and Antarctic Byrd ice cores; with the CO_2 record from gas enclosures in the Siple Dome, Taylor Dome and Byrd Antarctic ice cores; and with published alkenone and Mg/Ca SST records from nearby cold tongue cores ME0005A-24JC [*Kienast et al.*, 2006] and TR163–22 [*Lea et al.*, 2006] (Figure 1). Our composite alkenone ECT SST index (Figure 5d) is most consistent with the GISP-2 deglaciation timing (Figure 5a). Onset of equatorial warming at ~15 ka lags air temperature over Antarctica by several thousand years, and CO_2 by ~2 ka, and is coincident within dating uncertainty with the Bölling warming in northern high latitudes. This pattern is also evident in the individual alkenone SST records from V19–30 (Figure 5e) and from nearby core ME0005A-24JC (Figure 5f). Although the ~15 ka onset of warming appears as a distinct event, its amplitude is surprisingly small and only marginally rises above the natural variability present within the glacial interval. In core ME0005A-24JC (Figure 5f) and in the more northerly core KNR176-JPC32 from the Panama Basin (not shown) [*Pahnke et al.*, 2007] the ~15 ka warming step appears to terminate a brief cool excursion equivalent to Heinrich event 1, without significantly exceeding glacial background temperatures. From the perspective of these alkenone records it appears that the eastern Pacific region remained in glacial or near-glacial mode well into the termination. Between 11 and 12 ka our alkenone data reflect a sustained steep warming, matching within dating uncertainty the termination of the Younger Dryas. This warming constitutes the main deglacial warming signal, corresponding to ~2/3 of the total change in the composite SST index (Figure 5d).

4. Discussion

4.1. Evaluating the Role of the Oceanic Tunnel and CO_2

[15] These results have implications for identifying the mechanisms involved in the deglaciation process in the ECT region. Equatorial upwelling east of the Galapagos taps the deeper layers of the EUC [*Lukas*, 1986], which ultimately derive from subducting water masses in the subantarctic southwest Pacific [*Toggweiler et al.*, 1991; *Kessler*, 2006]. This transport pathway has long been considered an important mechanism for transmitting temperature anomalies from the Southern Ocean to the surface tropical Pacific where in turn they can affect global climate via tropical ocean-atmosphere teleconnections. By virtue of their location east of the Galapagos our cores are ideally situated to test the strength of this interior oceanic link (or "tunnel")

during the last termination. The transit time of water particles from the extratropics along subduction pathways is a few decades [*Toggweiler et al.*, 1991; *Goodman et al.*, 2005], essentially instantaneous within the resolution of the paleoceanographic records. Were this mechanism the dominant influence on eastern Pacific SST we would expect reconstructed temperatures to be phase locked with southern high-latitude climate without any apparent lag. As pointed out, the comparison between our ECT SST index and BYRD δ^{18}O temperature does not support this hypothesis. The onset of ECT warming lags BYRD δ^{18}O by $\sim$5 ka, with nearly half the deglacial warming in BYRD completed before ECT warming began. We conclude that, although this oceanic linkage mechanism may have operated during this time as suggested by thermocline carbon isotope signatures from the ECT [*Spero and Lea*, 2002], it was not the main control in shaping the pattern of equatorial Pacific warming. *Barker and Knorr* [2007] have suggested that the Antarctic climate signal during the last glacial period was globally pervasive and that the equatorial Pacific may have been central in its far-field propagation. At least over the deglaciation, the alkenone data question the effectiveness of this mechanism. Although the Antarctic climate signal may have reached the eastern equatorial Pacific through ocean advection, its signature was strongly modified by other dynamic processes. Further, the results do not support CO_2 as the main driver of the warming either. According to the Antarctic ice core records (Figure 5c) CO_2 rose by $\sim$40 ppm or half the G-I amplitude between 17 and 15 ka, prior to discernible warming in the eastern Pacific.

[16] These temporal relationships indicate that advection from the Southern Ocean and thermodynamic adjustment to CO_2 forcing are by themselves not sufficient to explain the deglacial SST response of the ECT. Instead the data imply that some other mechanism more closely attuned to Northern Hemisphere processes played a more prominent role. Coupled ocean atmosphere dynamics likely are the key to this link. Both the large annual cycle in this region and its interannual modulation by the ENSO involve strong dynamic coupling between the atmosphere and surface ocean. SST is sensitive to wind-induced divergent upwelling so that adjustments of the coupled system affecting the subsurface temperature structure or the upwelling rate could strongly influence SST. The resolution of our alkenone SST records is generally not sufficient to constrain the rapidity of the deglacial warming events, but their overall association with Greenland temperature suggests they were relatively abrupt. This is best seen in the individual SST records from V19–30 and ME0005A-24JC (Figures 5e and 5f). If so, they are more consistent with rapid dynamical adjustment rather than the more gradual process of advection from high latitudes or response to radiative forcing. In this rationale, the warming steps at $\sim$15 ka and $\sim$11.5 ka could have resulted from perturbations favoring either reduced upwelling, or a deepening of the equatorial thermocline (or both).

4.2. Relationship of the Eastern Tropical Pacific With the North Atlantic

[17] Were these adjustments communicated to this region from the North Atlantic? Or were they themselves the source of variability in the latter region? The evidence from the tropical Atlantic shows that during abrupt warming events such as the beginning of the Bölling and end of the Younger Dryas (YD), the tropical atmosphere adjusted with a northward shift of the marine ITCZ [*Peterson et al.*, 2000; *Haug et al.*, 2001]. However, this type of adjustment in the eastern Pacific (i.e., northward ITCZ shift) would be expected to strengthen the cross-equatorial southeast trade winds enhancing divergence and cooling, opposite to the observed pattern. We are thus confronted with modes of atmospheric adjustment during these events that appear different in the tropical Pacific and Atlantic. Seasonal forcing of the ITCZ today drives unidirectional responses in both basins (southward displacement in boreal winter) and therefore may not be a good analogy for the paleorecord. However, contrasting Atlantic-Pacific ITCZ movements occur today in association with ENSO events. During El Niño the ITCZ expands southward in the Pacific [*Deser and Wallace*, 1990] but is pulled northward in the western Atlantic because of positive SST anomalies there [*Enfield and Mayer*, 1997]. If ENSO-like adjustment was part of the communication mechanism between the North Atlantic, the tropical Atlantic, and the Pacific Oceans it would imply El Niño–like shifts during the Bölling and end-YD warming events, contrasting with the view that El Niño–like conditions prevailed in the cold Dansgaard-Oeschger stadials within the last glacial period [*Stott et al.*, 2002], and during the LGM [*Koutavas et al.*, 2002]. The results therefore question whether the analogy with ENSO is by itself an adequate framework for fully characterizing glacial and deglacial SST shifts in the equatorial Pacific.

[18] These results highlight the fundamental challenge of identifying and characterizing the elusive link between North Atlantic and tropical Pacific climate variability on a variety of timescales. The relationship between the two regions in the modern climate is just beginning to be understood and is far from a consensus view. Recent studies indicate that either of the two regions can act as a source of variability for the other. For example, *Hoerling et al.* [2001] attributed recent North Atlantic climate changes in part to a tropical Pacific origin, while *Dong et al.* [2006] demonstrated a mechanism through which warm North Atlantic SSTs in the positive phase of the Atlantic Multidecadal Oscillation can induce ENSO-damping atmospheric teleconnections. Modeling by *Sutton and Hodson* [2007] further showed that basin-scale warming of the North Atlantic can induce seasonal anomalies in wind stress and surface heat and freshwater fluxes in the tropical Pacific, potentially influencing decadal and ENSO variability. In the case of glacial and deglacial climate events, the role of the thermohaline circulation (THC) must be explicitly considered as it is clearly a major perturbation in the North Atlantic region [*McManus et al.*, 2004]. Modeling shows that collapse of the THC can induce El Niño–like [*Dong and Sutton*, 2002] or dipole-like [*Zhang and Delworth*, 2005] SST anomalies in the ECT, and can further affect the character of interannual ENSO variability. *Timmermann et al.* [2005] described a mechanism via which a collapsed THC can suppress ENSO by deepening the mean Pacific thermocline, while in contrast *Dong and Sutton* [2007] have

found that a reduced THC can amplify ENSO variance. Although at present these studies do not converge on a consistent mechanistic framework linking the North Atlantic with the tropical Pacific they do indicate plausible pathways for close interaction. If the presence of abrupt warming events during deglaciation in the ECT were confirmed, it would imply an in-phase relationship and rapid signal transmission between the two regions. This in turn would favor a fast atmospheric rather than a slower oceanic connection, likely involving tropical reorganization of the wind field affecting eastern Pacific upwelling.

4.3. Comparison of Alkenones With Mg/Ca

[19] One important issue that needs to be addressed is the divergence between alkenone and Mg/Ca temperature reconstructions from this region. As an example the high-resolution Mg/Ca record from nearby core TR163–22 by *Lea et al.* [2006] is shown in Figure 5g for comparison with the $U_{37}^{K'}$ records shown in Figures 5d, 5e, and 5f. The warming in the Mg/Ca reconstruction begins and peaks much earlier, lending the record a noted resemblance with Antarctic climate. At face value the differences between the Mg/Ca and $U_{37}^{K'}$ results can lead to very different paleoceanographic interpretations over the deglaciation interval. The divergence of the Mg/Ca and alkenone SST trends during the Holocene is also enigmatic and may result from different seasons or depths of production of alkenone-synthesizing coccolithophorids and *G. ruber* foraminifera.

[20] The discrepancy between the $U_{37}^{K'}$ and Mg/Ca methods in this ocean region has previously been noted by *Mix* [2006], who enumerated various potential sources of artifacts acting to alter the true temperature signal in either method. These include possible influences of nutrient or light stress on $U_{37}^{K'}$ values [*Prahl et al.*, 2006] and time-dependent calcite preservation/dissolution overprints on Mg/Ca that are difficult to correct for. More recently attention has been called to large differences between Mg/Ca results obtained with standard bulk measurement or flow-through time-resolved analysis methods [*Klinkhammer et al.*, 2007]. Some studies are further suggesting that the dependence of Mg/Ca on seawater salinity, previously thought to be minor, may have been underestimated [*Ferguson et al.*, 2008; *deMenocal et al.*, 2007]. The role of salinity deserves special scrutiny as it may help reconcile the $U_{37}^{K'}$ and Mg/Ca discrepancy over the critical interval of early deglaciation (19–15 ka). If H-1 cooling within this interval [*Kienast et al.*, 2006] was accompanied by upwelling of salty thermocline waters, then the resulting salinity increase might in part account for the strong increase in Mg/Ca ratios. Given the above considerations on proxy fidelity and divergence it seems imprudent to consider either proxy as superior and is instead important to view and evaluate each reconstruction carefully.

5. Conclusions

[21] In this study, we have combined alkenone results from five different sites from reasonably diverse depositional settings within the equatorial Pacific cold tongue, and have found that a composite SST record based on those is coherent with independent $U_{37}^{K'}$ reconstructions of the last deglaciation from two nearby sites [*Kienast et al.*, 2006; *Pahnke et al.*, 2007]. This adds to our confidence that the data capture the fundamental pattern of the deglacial temperature sequence in the eastern equatorial Pacific and that the latter essentially conforms to a Northern Hemisphere tempo. The implication is that the region's deglacial evolution involved coupled ocean-atmosphere dynamic adjustments, rather than passively reflecting climate signals and water properties acquired at high southern latitudes and traveling equatorward through the ocean interior. Given the dynamic character of the ECT region it is not surprising that a precise agreement with atmospheric CO_2 is not observed in the deglacial SST pattern. These results do not negate the overall significance of oceanic linkages or of radiative forcing as essential climate processes, but they do suggest an overarching role for ocean-atmosphere coupling in this region, and point to an underlying in-phase relationship with major deglacial events in the Northern Hemisphere. The precise linkage mechanisms between the North Atlantic and eastern Pacific remain elusive. In light of significant challenges facing our best paleoceanographic proxies in this region substantial further effort is needed to gain a firm underpinning of the key processes at work, and of how exactly this globally important region behaved during the late Pleistocene glacial cycles.

[22] **Acknowledgments.** We thank two anonymous reviewers for thorough and constructive input on the paper. A. Koutavas was supported in part by the National Oceanic and Atmospheric Administration Climate and Global Change Fellowship Program administered by the University Corporation for Atmospheric Research. This material is based upon work supported by the National Science Foundation under grant 0624954. J. P. Sachs acknowledges the support of the Gary Comer Science and Education Foundation.

References

Ahn, J., M. Wahlen, B. L. Deck, E. J. Brook, P. A. Mayewski, K. C. Taylor, and J. W. C. White (2004), A record of atmospheric CO_2 during the last 40,000 years from the Siple Dome, Antarctica ice core, *J. Geophys. Res.*, *109*, D13305, doi:10.1029/2003JD004415.

Barker, S., and G. Knorr (2007), Antarctic climate signature in the Greenland ice core record, *Proc. Natl. Acad. Sci. U. S. A.*, *104*, 17,278–17,282, doi:10.1073/pnas.0708494104.

Benway, H. M., A. C. Mix, B. A. Haley, and G. P. Klinkhammer (2006), Eastern Pacific warm pool paleosalinity and climate variability: 0–30 kyr, *Paleoceanography*, *21*, PA3008, doi:10.1029/2005PA001208.

Blunier, T., and E. J. Brook (2001), Timing of millennial-scale climate change in Antarctica and Greenland during the last glacial period, *Science*, *291*, 109–112, doi:10.1126/science.291.5501.109.

Broecker, W. S. (2003), Does the trigger for abrupt climate change reside in the ocean or the atmosphere?, *Science*, *300*, 1519–1522, doi:10.1126/science.1083797.

Cane, M. A. (1998), A role for the tropical Pacific, *Science*, *282*, 59–61, doi:10.1126/science.282.5386.59.

Clement, A. C., and M. A. Cane (1999), A role for the tropical Pacific coupled ocean-atmosphere system on Milankovitch and millennial timescales. Part I: A modeling study of tropical Pacific variability, in *Mechanisms of Global Climate Change at Millennial Timescales*, *Geophys. Monogr. Ser.*, vol. 112, edited by P. U. Clark, R. S. Webb, and L. D. Keigwin, pp. 363–371, AGU, Washington, D. C.

Conte, M. H., M.-A. Sicre, J. C. Weber, S. Schulte, D. Schulz-Bull, and T. Blanz (2006), Global temperature calibration of the alkenone unsaturation index ($U_{37}^{K'}$) in surface waters and comparison with surface sediments, *Geochem. Geophys. Geosyst.*, *7*, Q02005, doi:10.1029/2005GC001054.

Dansgaard, W., et al. (1993), Evidence for general instability of past climate from a 250-kyr Greenland ice-core record, *Nature*, *364*, 218–220, doi:10.1038/364218a0.

deMenocal, P., J. A. Arbuszewski, A. Kaplan, and M. Bice (2007), Fidelity of $\delta^{18}O$ seawater estimates using foraminiferal shell Mg/Ca and $\delta^{18}O$, *Eos Trans. AGU*, *88*(52), Fall Meet. Suppl., Abstract PP41E–08.

Deser, C., and J. M. Wallace (1990), Large-scale atmospheric circulation features of warm and cold episodes in the tropical Pacific, *J. Clim.*, *3*, 1254–1281, doi:10.1175/1520-0442(1990)003<1254:LSACFO>2.0.CO;2.

Dong, B.-W., and R. T. Sutton (2002), Adjustment of the coupled ocean-atmosphere system to a sudden change in the thermohaline circulation, *Geophys. Res. Lett.*, *29*(15), 1728, doi:10.1029/2002GL015229.

Dong, B.-W., and R. T. Sutton (2007), Enhancement of ENSO variability by a weakened Atlantic thermohaline circulation in a coupled GCM, *J. Clim.*, *20*, 4920–4939, doi:10.1175/JCLI4284.1.

Dong, B.-W., R. T. Sutton, and A. A. Scaife (2006), Multidecadal modulation of El Niño–Southern Oscillation (ENSO) variance by Atlantic Ocean sea surface temperatures, *Geophys. Res. Lett.*, *33*, L08705, doi:10.1029/2006GL025766.

Enfield, D. B., and D. A. Mayer (1997), Tropical Atlantic sea surface temperature variability and its relation to El Niño–Southern Oscillation, *J. Geophys. Res.*, *102*, 929–946, doi:10.1029/96JC03296.

Faul, K. L., A. C. Ravelo, and M. L. Delaney (2000), Reconstructions of upwelling, productivity, and photic zone depth in the eastern equatorial Pacific Ocean using planktonic foraminiferal stable isotopes and abundances, *J. Foraminiferal Res.*, *30*, 110–125, doi:10.2113/0300110.

Ferguson, J. E., G. M. Henderson, M. Kucera, and R. E. M. Rickaby (2008), Systematic change in foraminiferal Mg/Ca rations across a strong salinity gradient, *Earth Planet. Sci. Lett.*, *265*, 153–166, doi:10.1016/j.epsl.2007.10.011.

Fritts, H. C. (1976), *Tree Rings and Climate*, Elsevier, San Diego, Calif.

Goodman, P. J., W. Hazeleger, P. deVries, and M. Cane (2005), Pathways into the Pacific equatorial undercurrent: A trajectory analysis, *J. Phys. Oceanogr.*, *35*, 2134–2151, doi:10.1175/JPO2825.1.

Grootes, P. M., and M. Stuiver (1997), Oxygen 18/16 variability in Greenland snow and ice with 10^3–10^5-year time resolution, *J. Geophys. Res.*, *102*, 26,455–26,470, doi:10.1029/97JC00880.

Haug, G. H., K. A. Hughen, D. M. Sigman, L. C. Peterson, and U. Röhl (2001), Southward migration of the Intertropical Convergence Zone through the Holocene, *Science*, *293*, 1304–1308, doi:10.1126/science.1059725.

Hoerling, M. P., J. W. Hurrell, and T. Xu (2001), Tropical origins of recent North Atlantic climate change, *Science*, *292*, 90–92, doi:10.1126/science.1058582.

Horikawa, K., M. Minagawa, M. Murayama, Y. Kato, and H. Asahi (2006), Spatial and temporal sea-surface temperatures in the eastern equatorial Pacific over the past 150 kyr, *Geophys. Res. Lett.*, *33*, L13605, doi:10.1029/2006GL025948.

Kessler, W. S. (2006), The circulation of the eastern tropical Pacific: A review, *Prog. Oceanogr.*, *69*, 181–217, doi:10.1016/j.pocean.2006.03.009.

Kienast, M., S. S. Kienast, S. E. Calvert, T. I. Eglinton, G. Mollenhauer, R. François, and A. C. Mix (2006), Eastern Pacific cooling and Atlantic overturning circulation during the last deglaciation, *Nature*, *443*, 846–849, doi:10.1038/nature05222.

Klinkhammer, G. P., A. C. Mix, B. J. De Baere, and B. A. Haley (2007), High-quality proxy data from foraminiferal calcite using flow-through time resolved analysis, *Eos Trans. AGU*, *88*(52), Fall Meet. Suppl., Abstract PP41E–05.

Koutavas, A. (2003), Sea surface temperature variability in the eastern equatorial Pacific during the last deglaciation: Multiproxy geochemical reconstructions, Ph.D. thesis, Columbia Univ., New York, N. Y.

Koutavas, A., and J. Lynch-Stieglitz (2003), Glacial-interglacial dynamics of the eastern equatorial Pacific cold tongue–Intertropical Convergence Zone system reconstructed from oxygen isotope records, *Paleoceanography*, *18*(4), 1089, doi:10.1029/2003PA000894.

Koutavas, A., J. Lynch-Stieglitz, T. M. Marchitto, and J. P. Sachs (2002), El Niño–like pattern in ice age tropical Pacific sea surface temperature, *Science*, *297*, 226–230, doi:10.1126/science.1072376.

Lea, D. W. (2004), The 100,000-yr cycle in tropical SST, greenhouse forcing, and climate sensitivity, *J. Clim.*, *17*, 2170–2178, doi:10.1175/1520-0442(2004)017<2170:TYCITS>2.0.CO;2.

Lea, D. W., D. K. Pak, C. L. Belanger, H. J. Spero, M. A. Hall, and N. J. Shackleton (2006), Paleoclimate history of Galapagos surface waters over the last 135,000 yr, *Quat. Sci. Rev.*, *25*, 1152–1167, doi:10.1016/j.quascirev.2005.11.010.

Leduc, G., L. Vidal, K. Tachikawa, F. Rostek, C. Sonzogni, L. Beaufort, and E. Bard (2007), Moisture transport across Central America as a positive feedback on abrupt climate changes, *Nature*, *445*, 908–911, doi:10.1038/nature05578.

Liu, Z., and T. D. Herbert (2004), High-latitude influence on the eastern equatorial Pacific climate in the early Pleistocene epoch, *Nature*, *427*, 720–723, doi:10.1038/nature02338.

Liu, Z., and H. Yang (2003), Extratropical control of tropical climate, the atmospheric bridge and oceanic tunnel, *Geophys. Res. Lett.*, *30*(5), 1230, doi:10.1029/2002GL016492.

Locarnini, R. A., A. V. Mishonov, J. I. Antonov, T. P. Boyer, and H. E. Garcia (2006), *World Ocean Atlas 2005*, vol. 1, *Temperature*, *NOAA Atlas NESDIS*, vol. 61, edited by S. Levitus, 182 pp., NOAA, Silver Spring, Md.

Lukas, R. (1986), The termination of the equatorial undercurrent in the eastern Pacific, *Prog. Oceanogr.*, *16*, 63–90, doi:10.1016/0079-6611(86)90007-8.

McManus, J. F., R. Francois, J.-M. Gherardi, L. D. Keigwin, and S. Brown-Leger (2004), Collapse and rapid resumption of Atlantic meridional circulation linked to deglacial climate changes, *Nature*, *428*, 834–837, doi:10.1038/nature02494.

Mitchell, T. P., and J. M. Wallace (1992), The annual cycle of equatorial convection and sea surface temperature, *J. Clim.*, *5*, 1140–1156, doi:10.1175/1520-0442(1992)005<1140:TACIEC>2.0.CO;2.

Mix, A. (2006), Running hot and cold in the eastern equatorial Pacific, *Quat. Sci. Rev.*, *25*, 1147–1149, doi:10.1016/j.quascirev.2006.03.008.

Mix, A., N. G. Pisias, R. Zahn, W. Rugh, C. Lopez, and K. Nelson (1991), Carbon 13 in Pacific deep and intermediate waters, 0–370 ka: Implications for ocean circulation and Pleistocene CO_2, *Paleoceanography*, *6*, 205–226, doi:10.1029/90PA02303.

Müller, P. J., G. Kirst, G. Ruhland, I. Von Storch, and A. Rosell-Mele (1998), Calibration of the alkenone paleotemperature index $U_{37}^{K'}$ based on core-tops from the eastern South Atlantic and the global ocean (60°N–60°S), *Geochim. Cosmochim. Acta*, *62*, 1757–1772, doi:10.1016/S0016-7037(98)00097-0.

Ninkovich, D., and N. J. Shackleton (1975), Distribution, stratigraphic position and age of ash layer "L" in the Panama Basin region, *Earth Planet. Sci. Lett.*, *27*, 20–34, doi:10.1016/0012-821X(75)90156-9.

Pahnke, K., J. P. Sachs, L. Keigwin, A. Timmermann, and S.-P. Xie (2007), Eastern tropical Pacific hydrologic changes during the past 27,000 years from D/H ratios in alkenones, *Paleoceanography*, *22*, PA4214, doi:10.1029/2007PA001468.

Pena, L., I. Cacho, P. Ferretti, and M. A. Hall (2008), El Niño–Southern Oscillation–like variability during glacial terminations and interlatitudinal teleconnections, *Paleoceanography*, *23*, PA3101, doi:10.1029/2008PA001620.

Peterson, L. C., G. H. Haug, K. A. Hughen, and U. Röhl (2000), Rapid changes in the hydrologic cycle of the tropical Atlantic during the last glacial, *Science*, *290*, 1947–1951, doi:10.1126/science.290.5498.1947.

Prahl, F. G., L. A. Muehlhausen, and D. L. Zahnke (1988), Further evaluation of long-chain alkenones as indicators of paleoceanographic conditions, *Geochim. Cosmochim. Acta*, *52*, 2303–2310, doi:10.1016/0016-7037(88)90132-9.

Prahl, F. G., A. C. Mix, and M. A. Sparrow (2006), Alkenone paleothermometry: Biological lessons from marine sediment records off western South America, *Geochim. Cosmochim. Acta*, *70*, 101–117, doi:10.1016/j.gca.2005.08.023.

Sachs, J. P., and S. J. Lehman (1999), Subtropical Atlantic temperatures 60,000 to 30,000 years ago, *Science*, *286*, 756–759, doi:10.1126/science.286.5440.756.

Shackleton, N. J. (2000), The 100,000-year ice-age cycle identified and found to lag temperature, carbon dioxide, and orbital eccentricity, *Science*, *289*, 1897–1902, doi:10.1126/science.289.5486.1897.

Smith, H. J., H. Fischer, D. Mastroianni, B. Deck, and M. Wahlen (1999), Dual modes of the carbon cycle since the Last Glacial Maximum, *Nature*, *400*, 248–250, doi:10.1038/22291.

Spero, H. J., and D. W. Lea (2002), The cause of carbon isotope minimum events on glacial terminations, *Science*, *296*, 522–525, doi:10.1126/science.1069401.

Stott, L., C. Poulsen, S. Lund, and R. Thunell (2002), Super ENSO and global climate oscillations at millennial timescales, *Science*, *297*, 222–226, doi:10.1126/science.1071627.

Sutton, R. T., and D. L. R. Hodson (2007), Climate response to basin-scale warming and cooling of the North Atlantic Ocean, *J. Clim.*, *20, 891–907, doi:10.1175/JCLI4038.1.*

Timmermann, A., S.-I. An, U. Krebs, and H. Goosse (2005), ENSO suppression due to a weakening of the North Atlantic thermohaline circulation, *J. Clim.*, *18*, 3122–3139, doi:10.1175/JCLI3495.1.

Toggweiler, J. R., K. Dixon, and W. S. Broecker (1991), The Peru upwelling and the ventilation of the South Pacific thermocline, *J. Geophys. Res.*, *96*, 20,467–20,497, doi:10.1029/91JC02063.

Tyrrell, T., and A. Merico (2004), *Emiliania huxleyi*: Bloom observations and the conditions that induce them, in *Coccolithophores — From Molecular Processes to Global Impact*, edited by H. R. Thierstein and J. R. Young, pp. 75–97, Springer, New York.

Tyrrell, T., and A. H. Taylor (1996), A modeling study of *Emiliania huxleyi* in the NE Atlantic, *J. Mar. Syst.*, *9*, 83–112, doi:10.1016/0924-7963(96)00019-X.

Wang, C., and P. C. Fiedler (2006), ENSO and the eastern tropical Pacific: A review, *Prog. Oceanogr.*, *69*, 239–266, doi:10.1016/j.pocean.2006.03.004.

Zhang, R., and T. L. Delworth (2005), Simulated tropical response to a substantial weakening of the Atlantic thermohaline circulation, *J. Clim.*, *18*, 1853–1860, doi:10.1175/JCLI3460.1.

A. Koutavas, Department of Engineering Science and Physics, College of Staten Island, City University of New York, 2800 Victory Boulevard, New York, NY 10314, USA. (koutavas@mail.csi.cuny.edu)

J. P. Sachs, School of Oceanography, University of Washington, Box 355351 (OSB 521), Seattle, WA 98195, USA.